ELSEVIER

Journal of Hazardous Materials B101 (2003) 157–177

Journal of Hazardous Materials

www.elsevier.com/locate/jhazmat

Study of the spread of a cold instantaneous heavy gas release with surface heat transfer and variable entrainment

Ashok Kumar*, Abjheet Mahurkar, Amit Joshi

Department of Civil Engineering, University of Toledo, 2801 W. Bancroft Street, Toledo, OH 43606, USA

Received 23 January 2002; received in revised form 27 May 2003; accepted 28 May 2003

Abstract

Air quality models help in developing relationships between the amount of pollutant released into the ambient atmosphere by a source and the corresponding incremental contribution in the atmospheric concentration. Of the various dispersion models, the heavy gas models help in predicting the concentrations due to release of gases heavier than air and the risks associated with the increased concentrations. Several differences exist among the various models developed to study the heavy-gas dispersion phenomena. These differences mainly arise because of the varied treatment given to physical processes involved in the dispersion mechanism. One of these processes, which have not been fully considered in many of the existing models, is the effect of ground heating on the movement of a cloud under windy conditions. In this study, the box model developed by Kunsch and Fannelop [J. Hazard. Mater. 43 (1995) 169] is extended to incorporate variable air entrainment on the dispersion of a heavy gas cloud spreading in a channel under windy conditions. The air entrainment was assumed to be proportional to the cloud frontal velocity. The semi-analytical equations developed were then solved by numerical methods to provide a heavy gas cloud dispersion profile. The popular Runge-Kutta fourth order technique was adopted to solve the differential equations numerically. The model was applied on a cold cloud released instantaneously and the results indicated that the model behavior follows closely the expected dispersion trends and observed cloud characteristics reported in a laboratory study. The trial run carried out in order to model the scenario of no heat transfer, by equating the source temperature to the ambient temperature, followed variations observed in the field. The analysis of cloud behavior indicated that the cloud length is strongly influenced by source density and initial cloud temperature.

Keywords: Heavy gas; Dispersion model; Surface heat transfer; Entrainment; Cloud temperature

* Corresponding author. Tel.: +1-419-530-8136; fax: +1-419-530-8116.
E-mail address: akumar@utnet.uroledo.edu (A. Kumar).

0304-3894/$ – see front matter © 2003 Elsevier B.V. All rights reserved.
doi:10.1016/S0304-3894(03)00171-7

Nomenclature

a	thermal diffusivity
A	surface area of the cloud at the top and bottom of cloud
B	width of the channel
B_i	Biot number ($B_i = \alpha L_{\mathrm{ref}}/\lambda_{\mathrm{w}}$)
c	concentration (mass)
c_1, c_2	constants in the Fay and Ranck's [12] equation
c_{p}, c_{pa}, c_{ps}	specific heat of gas (mixture, ambient, source)
C_{f}	wave velocity ($C_{\mathrm{f}} = \sqrt{[(\rho_{\mathrm{c}} - \rho_{\mathrm{a}})/\rho_{\mathrm{c}}]\,gh}$)
Fo	Fourier number ($Fo = at_{\mathrm{ref}}/L^2_{\mathrm{ref}}$)
Fr	densimetric Froude number ($Fr = U_{\mathrm{f}}/C_{\mathrm{f}} = (k\rho_{\mathrm{s}}/\rho_{\mathrm{a}})^{1/2}$)
g	acceleration due to gravity
h	height of the cloud
k	empirical constant in the frontal condition
m, m_{a}, m_{s}	total mass of the cloud, mass of air, mass of gas in the cloud
$\dot{m}_{\mathrm{a}}$, $\dot{m}_{\mathrm{s}}$	mass-flow rate of entrained air and of the source, respectively
Q_{s}	volume of gas in the cloud (per unit width)
$\dot{Q}_{\mathrm{s}}$	volume flow rate of the source (per unit width)
R, R_{a}, R_{s}	gas constant of the cloud, the ambient air and the source
Ri	Richardson number
St	Stanton number ($\mathrm{St} = \alpha/\rho_{\mathrm{s}}c_{\mathrm{ps}}C_{\mathrm{ref}}$)
t	time
T	temperature in the ground surface
T_{c}, T_{a}, T_{s}	temperature of the cloud, the ambient air and the source
T_{w}	temperature of the surface of contact
u^*	friction velocity
U_{f}	velocity of the cloud front
U_{c}, U_{w}	cloud and ambient wind speeds, respectively
U_{e}, U_{t}	edge entrainment and top entrainment velocity, respectively
v_{e}	entrainment velocity
V	volume of the dispersing cloud
V_{s}, V_{a}	volume of the source gas and volume of entrained ambient air in the cloud
V_{e}, V_{t}	flow rate of entrained air from the edge and top of the cloud, respectively
$\dot{V}_{\mathrm{s}}$, $\dot{V}_{\mathrm{a}}$	volume flow rate of the source and the ambient air entrained into the cloud
X_{f}	location of the cloud front
y	coordinate normal to the ground surface

Greek letters

α	heat-transfer coefficient
α_{e}	air entrainment coefficient
β_{c}	constant to account for the non-uniformity of the flow field over the cloud surface
δ	penetration depth of a temperature perturbation

λ_w	thermal conductivity of the surface on which the cloud spreads
λ	thermal conductivity of the cloud
Ω	$1/3B_i\delta(t)$ (time parameter)
ρ_c, ρ_a, ρ_s	density of the cloud, the ambient air and the source
τ_T, τ_G	shear stresses at the top and bottom of the cloud

Subscripts/superscripts

a	ambient
c	cloud
f	front property
s	source
ref	reference quantity
w	property of the surface on which cloud spreads
$(\bar{})$	dimensionless quantity

1. Introduction

The development of new technologies requires the industrial use of dangerous substances that can be toxic, inflammable or explosive. Some of these substances when released into air can behave as gases heavier than air. The main causes for this behavior are [1]:

- The molecular weight of released material is greater than that of air (e.g. chlorine).
- The density is greater than that of air due to the low temperature of release (e.g. liquefied natural gas).
- The density is greater than that of air also for compounds with lower molecular weight due to their storage conditions.
- The density is greater than that of air due to the chemical reactions between the substance released and the atmospheric water vapor.

Due to the above-mentioned characteristic of heavy gases, they tend to disperse within the surface area close to the ground. Several accidents due to release of toxic heavy gases have led to loss in human life. Tragedies in Bhopal, India, in 1985, and Mississauga, in 1979, have drawn attention to the need for better emergency planning to avert the undesirable outcome of toxic releases. Driven by the efforts of the industry to prevent and mitigate such incidents, modeling episodic releases of hazardous or toxic materials has rapidly evolved in the past few decades. The increase in the use of heavy gases for industrial purposes has resulted in the development of several mathematical models to predict the integrated characteristics of a heavy gas cloud. Dense gas models are important components of emergency response systems as well as important tools for environmental impact assessments and risk assessments. The wide use of these models in the industry has led to the development of more accurate and complex models. These models can be classified into three principal groups [2]:

(A) Box (Slab) models, which are the most popular of the three types, essentially treat the cold heavy gas as a cylinder of uniform properties. The mass transfer is assumed to

occur by entrainment across the density interface of the cloud and is assumed to depend on turbulence levels, density differences and cloud speed.

(B) The second type of models which are widely recognized are the depth averaged (K-theory) models. These models suitably integrate simplified equations of mass, momentum, and energy conservation, in either two- or three-dimensional form. In most of these models, mass transfer is assumed to be dependent on a density gradient (Richardson number).

(C) The third class of models includes the three-dimensional (3D) conservation equations. These are complex numerical models employing 3D partial differential equations describing conservation of mass, momentum and energy.

One must bear in mind that if a simple model is able to capture the basic plume thermodynamics accurately it may perform as well as more complex models as indicated by the study done by Hanna et al. [3].

The dispersing cloud of a heavy gas release can be divided into three major phases:

(A) an initial gravity dominated phase or slumping phase;
(B) the transition phase; and
(C) the buoyancy dominated phase.

The phases are depicted in Fig. 1 for illustrative purposes. The dispersion of heavy gases into the atmosphere has some characteristics that differentiate it from that of passive gases. The initial phase of dispersion is characterized by collapsing of the cloud due to a negative buoyant force. As the cloud collapses it entrains air due to internal turbulence, becomes dilute and also entrains momentum. This phase is characterized by an increase in the radius and volume of the cloud and decrease in its height. Meanwhile the Richardson number, the ratio of cloud potential energy to ambient turbulent energy [4], decreases that results in the external ambient turbulence penetrating the relatively stable dense cloud. Gradually the cloud is transformed into a passive cloud. This transition to a neutral density occurs as the cloud's Richardson number falls below a critical value.

The purpose of this study is to develop an improved box model, which considers the complex phenomena of heat transfer, air entrainment and ambient wind speed effects. A brief account on various kinds of models and comparison among them is given below.

Among the numerous models for the dispersion of heavy gases there exist substantial differences regarding the way various important physical phenomena are treated by the

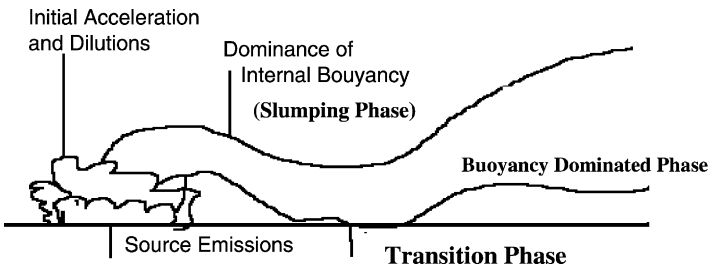

Fig. 1. Stages in the dispersion of a dense gas release.

model [4]. A common ground has still not been reached among the various developers on how to model accurately the important phenomena like air entrainment [4,5], the cloud translation speed [6], transition to passive dispersion phase [4], and the importance of heat transfer effects from the ground and entrained air [7]. Moreover, the box models have still not performed satisfactorily in near calm (stable) conditions [8] and few box models take complex terrain into consideration [5].

Heavy gas model code (equation) comparison exercises have found that there still exist substantial differences between the model codes, even when these codes have been parameterized using essentially the same experimental data [8]. Even the complex 3D unsteady state models developed show only a discrete agreement between the measured and calculated values on preliminary comparison with experimental data and call for continuation of the study and further development of the models [2].

The reviews by Wheatley et al. [9] and Britter [1] indicated there is no consensus as to which entrainment expression is the best. Gudiwaka [6] suggested that incorporating a better entrainment expression, especially for calm-wind conditions, could make improvements to his model.

The salient features of the above models, which have been considered in the development of the proposed model, are described below.

Gudiwaka [6] in his box model has improved upon the modeling of the motion of the cloud compared to the erroneous modeling of the cloud movement earlier, which led to a much faster cloud travel time than observed. He has taken into consideration the significant inertia effect of the cloud, which has to accelerate from its initial position to reach a constant advection velocity after a certain time. The integral equation developed by Wheatley and Prince [10] for the translation motion of a heavy gas cloud has been used in this model. This model, which is a simple box type, estimates the dispersion of instantaneous releases of dense gases. The model was calibrated using the Thorney Island data, which showed the edge entrainment coefficient to be zero and only top entrainment being substantial. This model did not consider the effects of heat transfer on the dispersion and of ambient wind speed on the entrainment.

The model developed by Kunsch and Fannelop [7] considered the effect of the heat transfer on the cloud. However, this was only in no wind conditions and hence the model was not applied to predict the cloud behavior in windy conditions. The effect of heat was considered on the concentration, front velocity and position of the cloud. Moreover, this model based its entrainment rate on shallow layer code and assumed it equal to a constant value of 0.007 m/s. The model assumed a rectangular cloud profile and developed the equations for unit width of the cloud for both instantaneous and continuous release of the gas. Later, Nielsen and Ott [11] suggested that heat transfer from the ground sometimes reduces the density effect induced by the enthalpy deficit. They showed that the surface heat flux decreased by 38% during a 3 min long release period using Desert tortoise measurements.

Fay and Ranck [12] also developed a model in which they expressed the entrainment in terms of the ambient wind speed. The expression given by them based on experimental observations assumes negligible edge entrainment and expresses the top entrainment in terms of friction velocity for both isothermal and non-isothermal conditions.

The study attempts to incorporate into the basic box model, the equations for ground heat transfer as developed by Kunsch and Fannelop [7] and expression for cloud advection

velocity given by Wheatley and Prince [10]. The literature review found that there was no uniformity regarding the consideration of air entrainment phenomena among the models. Some models adopted the front velocity as the governing factor while other models used ambient velocity. The study will model the entrainment of ambient air by assuming it proportional to the frontal velocity.

Thus, the resulting model will be applicable for instantaneous releases of heavy gases spreading in a channel under windy conditions, while considering the heat transfer and cloud inertia effects on the dispersion of the gas and incorporating a suitable entrainment expression. The resulting model will be compared for characteristic cloud behavior by conducting trial runs. The cloud response under various input conditions will also be studied. The dispersion trends for no heat-transfer conditions will be analyzed and sensitivity analysis performed to identify which model inputs have the maximum impact on the calibration and conclusions of the model results.

2. Model development

This section presents the formulation of the proposed dispersion model for an instantaneous heavy gas release. A basic box model is constructed based on the assumptions given below. The governing equations are developed by a step-by-step process and are re-expressed in non-dimensional terms. A semi-analytical solution for the formulation equations is generated, which helps in portraying the effects of various parameters on the cloud dispersion characteristics.

The basic assumptions, which have been made to simplify the model, are as follows:

(A) The dispersing cloud moves over flat terrain or water.
(B) The surface has constant roughness.
(C) There are no obstructions to the wind or moving cloud.
(D) The contaminant gas undergoes no chemical or physical reaction during dispersion.
(E) Spatial variations in the dependent variables are neglected. The density and temperature of the spreading cloud are supposed to be dependent only on time.
(F) Local concentration fluctuations are not predicted, i.e. spatial invariance in the direction of spreading is assumed.
(G) The initial temperature of the surface on which the cloud spreads is assumed to be equal to the ambient temperature.
(H) Entrainment of ambient air from the edges of the cloud is negligible.

2.1. Model formulation

A rectangular cloud of initial length, X_f, height, h, and width, B, with temperature profile as shown in Fig. 2, is assumed. The formulated model is a modified form of the model proposed by Kunsch and Fannelop [7].

The equation of energy conservation in the cloud can be expressed as:

$$M\,c_p\left(\frac{dT_c}{dt}\right) = \rho_s \dot{V}_s c_{ps}(T_s - T_c) + \rho_a \dot{V}_a c_{pa}(T_a - T_c) + \alpha(T_w - T_c)B\,X_f \qquad (2.1)$$

The three terms on RHS of the above expression represent the heat flux from the source, the entrained air and the ground, respectively.

The unsteady heat conduction in the surface on which the cloud spreads is assumed to be represented by an one-dimensional Fourier equation and has boundary layer characteristics; hence, can be represented as:

$$\int_0^{\delta} \frac{\partial T}{\partial t} \mathrm{d}y = \int_0^{\delta} a \frac{\partial^2 T}{\partial y^2} \mathrm{d}y \tag{2.2}$$

This assumption may not hold very well for the spreading front of the cloud and for free advection clouds. Future experimental work will clarify the use of the above equation. On substituting the profile as:

$$\left(\frac{T}{T_\mathrm{a}} - 1\right) = \left(\frac{T_\mathrm{w}}{T_\mathrm{a}} - 1\right)(1-\eta)^3 \tag{2.3}$$

from Fig. 2, where $\eta = y/\delta$, we obtain:

$$\frac{\mathrm{d}}{\mathrm{d}t}[\delta(T_\mathrm{w} - T_\mathrm{a})] = 12a\frac{T_\mathrm{w} - T_\mathrm{a}}{\delta} \tag{2.4}$$

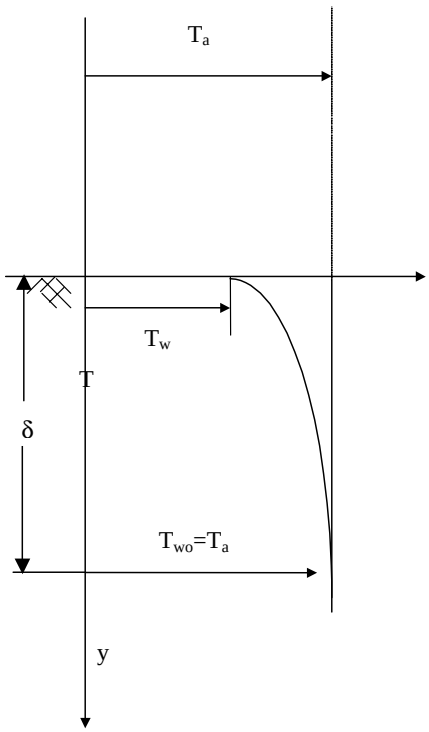

Fig. 2. Idealized temperature profile in the ground.

Equating the heat flux from heat transfer to the heat flux due to conduction we have:

$$\lambda_w \left.\frac{\partial T}{\partial y}\right|_{y=0} = \alpha(T_w - T_c) \tag{2.5}$$

The above coupling condition can be written in terms of the assumed similarity profile, given by Eq. (2.4), as:

$$T_w - T_a = -\frac{\alpha\delta}{3\lambda_w}(T_w - T_c) \tag{2.6}$$

The concentration of the cloud is defined as $c = m_s/m$, where m the total cloud mass is equal to the sum of the entrained air mass (m_a) and the initial undiluted gas mass (m_s). Therefore, $m = m_s + m_a$. An expression for rate of change of concentration can be obtained on differentiating the expression:

$$c = \frac{m_s}{m_s + m_a} \tag{2.7}$$

as:

$$\frac{dc}{dt} = c\frac{\dot{m}_s}{m_s} - c^2\frac{\dot{m}}{m_s} \tag{2.8}$$

This set of equations is completed by the standard box model equation for the frontal velocity based on gravity–current relation commonly used in most of the models developed, given as:

$$U_f = \frac{dX_f}{dt} = \left(kg\frac{\rho_c - \rho_a}{\rho_a}h\right)^{1/2} = \left(k\frac{\rho_c}{\rho_a}\right)^{1/2} C_f \tag{2.9}$$

In the above equation it is assumed that plume width does not increase as the cloud travels downwind.

2.2. Dimensionless equations

The equations given above are expressed in non-dimensional terms with the help of suitable scaling variables. In the case of instantaneous releases the scaling parameters chosen by Kunsch and Fannelop [7] are as follows:

(A) An appropriate reference length, $L_{ref} = h(t = 0)$, which is the initial height of the cloud;
(B) A suitable reference speed taken as the propagation velocity corresponding to the fictious layer height: $C_{ref} = (gL_{ref})^{1/2}$;
(C) A corresponding reference time $t_{ref} = L_{ref}/C_{ref}$; and
(D) The ambient temperature adopted as the reference temperature.

The above scaling variables are used for a non-dimensional representation of the model equations given in the earlier section. The modified expressions obtained are as follows:

On being combined, Eqs. (2.4) and (2.6) give the relationship for the rate of change for the penetration depth as:

$$\frac{\mathrm{d}}{\mathrm{d}\bar{t}}(\bar{\delta}^2) = \frac{1+\Omega}{2+\Omega}\left[24Fo - 2\bar{\delta}^2\frac{1}{\bar{T}_\mathrm{c}-1}\frac{\mathrm{d}\bar{T}_\mathrm{c}}{\mathrm{d}t}\right] \quad \text{with} \quad \Omega(\bar{t}) = \frac{1}{3}Bi\,\bar{\delta}(\bar{t}) \tag{2.10}$$

The entrainment of air into a cloud is assumed to occur from the edges and the top of the cloud in case of both rectangular and cylindrical clouds. The general expression for air entrainment considering the above two components is:

$$\dot{V}_\mathrm{a} = V_\mathrm{e} + V_\mathrm{t} \tag{2.11}$$

In case of a rectangular cloud, the volume of entrained air from the top and the edges can be expressed in terms of the entrainment velocities as given below:

$$\dot{V}_\mathrm{a} = (2Bh + 2X_\mathrm{f}h)U_\mathrm{e} + X_\mathrm{f}BU_\mathrm{t} \tag{2.12}$$

As evident from the literature review, the various models give varying importance to the above two entrainment rates. In the models being developed, it is assumed that the entrainment contribution from the edges of the cloud is negligible when compared to the top entrainment. This assumption is based on the fact that greater area of the rectangular cloud is exposed to entrainment from the top in the initial stages of dispersion. Moreover, the results of the earlier models that carried out model calibrations with observed data, namely, Gudiwaka's [6] model, determined edge entrainment to be negligible on calibration with Thorney Island data. Also, Fay and Ranck [12] found the top entrainment to be the governing parameter in their model, based on field and wind tunnel studies. Considering the above assumption and denoting top entrainment velocity as v_e, one can reduce the entrainment equation to:

$$\dot{V}_\mathrm{a} = X_\mathrm{f}Bv_\mathrm{e} \tag{2.13}$$

Note that the above equation indicates that the dense gas is spreading in a channel ($\dot{V}_\mathrm{a} \propto X_\mathrm{f}$). In a "free" cloud, entrainment will be proportional to the square of cloud radius. Substituting the above expression, for unit width, i.e. $\dot{V}_\mathrm{a} = X_\mathrm{f}v_\mathrm{e}$ in Eq. (2.1), and on non-dimensionalizing, we get the expression for rate of change of cloud temperature as:

$$\frac{\mathrm{d}\bar{T}_\mathrm{c}}{\mathrm{d}\bar{t}} = c\frac{\dot{\bar{Q}}_\mathrm{s}}{\bar{Q}_\mathrm{s}}\frac{c_\mathrm{ps}}{c_\mathrm{p}}(\bar{T}_\mathrm{s}-\bar{T}_\mathrm{c}) - c\frac{\bar{X}_\mathrm{f}}{\bar{Q}_\mathrm{s}}\frac{c_\mathrm{ps}}{c_\mathrm{p}}\left[\left(\frac{\rho_\mathrm{a}}{\rho_\mathrm{s}}\right)\left(\frac{c_\mathrm{pa}}{c_\mathrm{ps}}\right)\bar{v}_\mathrm{e}(\bar{T}_\mathrm{c}-1) - St(\bar{T}_\mathrm{w}-\bar{T}_\mathrm{c})\right] \tag{2.14}$$

The rate of change of concentration with time is obtained from Eq. (2.8):

$$\frac{\mathrm{d}c}{\mathrm{d}\bar{t}} = c(1-c)\frac{\dot{\bar{Q}}_\mathrm{s}}{\bar{Q}_\mathrm{s}} - c^2\frac{X_\mathrm{f}}{\bar{Q}_\mathrm{s}}\left(\frac{\rho_\mathrm{a}}{\rho_\mathrm{s}}\right)\bar{v}_\mathrm{e} \tag{2.15}$$

And, finally, the expression for the position of the front is found from Eq. (2.9) and equation of state for ideal gas to be:

$$\frac{\mathrm{d}}{\mathrm{d}\bar{t}}(\bar{X}_\mathrm{f}^{3/2}) = \frac{3}{2}Fr\left[\left|1-\frac{\rho_\mathrm{a}}{\rho_\mathrm{c}}\right|\frac{1}{c}\bar{Q}_\mathrm{s}\right]^{1/2} \quad \text{with} \quad \frac{\rho_\mathrm{a}}{\rho_\mathrm{c}} = \left[(1-c)+c\left(\frac{R_\mathrm{s}}{R_\mathrm{a}}\right)\right]\bar{T}_\mathrm{c} \tag{2.16}$$

The relevant expressions for the dimensionless groupings are given in the Nomenclature.

2.3. Semi-analytical solution

In this section, the solution for the model is developed based on the basic expressions discussed in the earlier sections. Appropriate approximations are made, where necessary, to simplify the analytical solution. The main equations required to estimate the characteristics of cloud dispersion are also identified. The governing model equations based on the assumptions made earlier are discussed below:

In the case of instantaneous fixed-volume releases, i.e. $\bar{Q}_s = \bar{Q}_s(t=0)$ and $\mathrm{d}\bar{Q}_s/\mathrm{d}t = 0$, if in the first approximation we neglect heat transfer and air entrainment, the expression for front position is simplified to:

$$\bar{X}_{f_0} = \left(\frac{3}{2}Fr\right)^{2/3}\left(\frac{\rho_s - \rho_a}{\rho_s}\bar{Q}_s\right)^{1/3}(\bar{t}')^{2/3} = c_0(\bar{t}')^{2/3} \tag{2.17}$$

where the time shift introduced to take into account the initial position of front is:

$$\bar{t}' = \bar{t} + \bar{t}_0 = \bar{t} + \left[\frac{\bar{X}_f(t=0)}{c_0}\right]^{3/2}$$

In the expression for concentration given by Eq. (2.7), substituting the value of m_a after integrating the below equation:

$$\dot{m}_a = \rho_a B X_f v_e \cong \rho_a B X_{f_0} v_e \tag{2.18}$$

we get an improved result for concentration as given below, in which the value of X_{f_0} is obtained from Eq. (2.17):

$$c = \frac{\bar{m}_s}{\bar{m}} = \frac{1}{1 + (\bar{m}_a/\bar{m}_s)} = \frac{1}{1 + (\rho_a/\rho_s)(1/\bar{Q}_s)\int \bar{v}_e \bar{X}_f \,\mathrm{d}t} \tag{2.19}$$

Similarly, on approximating the penetration depth as $\bar{\delta} = (12Fo\bar{t})^{1/2}$, the expression for rate of cloud temperature with time is simplified to:

$$\frac{\mathrm{d}\bar{T}_c}{\mathrm{d}\bar{t}} = -c\frac{\bar{X}_{Fo}}{\bar{Q}_s}\left[\left(\frac{\rho_a}{\rho_s}\right)\bar{v}_e + \frac{St}{1+\Omega}\right](\bar{T}_c - 1) \tag{2.20}$$

The integration by parts of the above equation, when only first order terms are retained, gives:

$$\bar{T}_c - 1 = (\bar{T}_s - 1)c^A \quad \text{with} \quad A = 1 + \left(\frac{\rho_s}{\rho_a}\right)\frac{1}{\bar{v}_e}\frac{St}{(1+\Omega)} \tag{2.21}$$

The calculation of frontal position is given by:

$$\bar{X}_f^{3/2} = \bar{X}_f^{3/2}(t=0) + c_0^{3/2}\int_{\bar{t}_0}^{\bar{t}'}\left[\frac{(1-\rho_a/\rho_c)}{(1-\rho_a/\rho_s)}\frac{1}{c}\right]^{1/2}\mathrm{d}\bar{t}' \tag{2.22}$$

In the above equation, the density of the cloud mass is provided by the equation of state for ideal gas mixtures:

$$\frac{\rho_c}{\rho_a} = \frac{R_a T_a}{R T_c}$$

In the above expression, substituting for the gas constant per unit mass of mixture ($R = cR_s + (1-c)R_a$) and expressing cloud temperature in non-dimensional terms, one obtains:

$$\frac{\rho_a}{\rho_c} = \left[(1-c) + c\frac{R_s}{R_a}\right]\bar{T}_c \tag{2.23}$$

The frontal velocity of the cloud, represented as U_f, is given by:

$$\bar{U}_f = \frac{d\bar{X}_f}{d\bar{t}} = Fr\left[\left|1 - \frac{\rho_a}{\rho_c}\right| \frac{1}{c}\frac{\bar{Q}_s}{\bar{X}_f}\right]^{1/2} \tag{2.24}$$

The equation for cloud advection is adopted from the expression given by Wheatley and Prince [10] stated below. The value of β_c was determined to be 0.8 from experiments.

$$\frac{d(\rho_c V U_c)}{dt} = \rho_a \frac{dV}{dt}\left(\frac{\beta_c U_w + U_c}{2}\right) + A(\tau_T + \tau_G) \tag{2.25}$$

Assuming U_w to be a constant and that shear stress terms can be neglected in the early stages of cloud motion, a simplified expression for advection may be obtained. The simplified equation expressed in non-dimensional terms is given as:

$$\frac{d(\overline{\rho_c V U_c})}{d\bar{t}} = \bar{\rho}_a \frac{d\bar{V}}{d\bar{t}}\left(\frac{\beta_c \bar{U}_w + \bar{U}_c}{2}\right) \tag{2.26}$$

The Eqs. (2.19), (2.21)–(2.24) and (2.26) form the governing equations which can be solved by mathematical packages to give the required unknowns, namely cloud concentration, cloud temperature, cloud frontal position, cloud density, cloud front velocity, and cloud advection velocity, respectively. Thus, the six unknowns (represented as: c, T_c, X_f, ρ_c, U_f and U_c) are solved using the above-mentioned equations to provide a closed form solution. However, the relevant expression for top entrainment has not been considered, which is discussed in detail in the following Section 2.4.

2.4. Air entrainment expression

In Eqs. (2.19) and (2.21), the expression for top entrainment has not been substituted. The top entrainment is assumed proportional to the cloud frontal velocity as considered by many models including Gudiwaka [6], Van Ulden [13], Germeles and Drake [14], etc.

Thus top entrainment is given as:

$$v_e = \alpha_e U_f \tag{2.27}$$

Expressing the above equation in non-dimensional form we have:

$$\bar{v}_e = \alpha_e \bar{U}_f$$

Substituting for U_f from Eq. (2.24) we have:

$$\bar{v}_e = \alpha_e \frac{d\bar{X}_f}{d\bar{t}} = \alpha_e Fr \left[\left| 1 - \frac{\rho_a}{\rho_c} \right| \frac{1}{c} \frac{\bar{Q}_s}{\bar{X}_f} \right]^{1/2} \tag{2.28}$$

Substituting the above entrainment expression in the equations derived earlier we get expressions in terms of the unknown cloud variables. These expressions can then be solved by numerical methods to give the values of important cloud properties. The steps involved in the numerical solution are discussed in Section 3.

3. Numerical solution

A numerical solution involves initialization of few of the model parameters, and then using an iterative (step-by-step) procedure, which estimates the values of the variables at an incremented step. The equations derived in the earlier Section 2.4 can be rearranged to develop a new set of expressions compatible to numerical analysis.

Eq. (2.24) gives a simple differential relationship for X_f, which can be solved by the Runge-Kutta method by assuming suitable initial values for X_f, c and ρ_c. The equation repeated here for convenience is:

$$\frac{d\bar{X}_f}{d\bar{t}} = Fr \left[\left| 1 - \frac{\rho_a}{\rho_c} \right| \frac{1}{c} \frac{\bar{Q}_s}{\bar{X}_f} \right]^{1/2} \tag{3.1}$$

Eq. (2.20) can be used for determining temperature of the cloud (T_c) after initializing the values of T_c, c, v_e and time step t. In the equation, Ω can be rewritten as follows:

$$\Omega = \frac{1}{3} Bi\bar{\delta} \approx \frac{\alpha}{b}\sqrt{\bar{t}} \quad \text{with} \quad b = \sqrt{\lambda_w \rho_w c_w}$$

In the case of good conductors with large heat capacities, b is large and hence we can approximate the above equation, which is accurate for most common gas cloud/surface materials, as:

$$1 + \Omega \approx 1 + \varepsilon\sqrt{\bar{t}} \quad \text{with} \quad \varepsilon \ll 1$$

The value of $\varepsilon \ll 0.01$ is satisfied for concrete, metals, etc. The above condition is not fulfilled in case of good insulators [7]; hence, this approximate solution is not recommended. Substituting the above relation in Eq. (2.20), we have:

$$\frac{d\bar{T}_c}{d\bar{t}} = -c \frac{\bar{X}_{Fo}}{\bar{Q}_s} \left[\left(\frac{\rho_a}{\rho_s} \right) \bar{v}_e + \frac{St}{1 + \varepsilon\sqrt{\bar{t}}} \right] (\bar{T}_c - 1) \tag{3.2}$$

We can determine concentration from Eq. (2.19) after substituting for v_e as expressed in first part of Eq. (2.28). Thus, we get:

$$c = \frac{1}{1 + (\rho_a/\rho_s)(1/\bar{Q}_s) \int \bar{v}_e \bar{X}_f \, dt} = \frac{1}{1 + (\rho_a/\rho_s)(1/\bar{Q}_s) \int \alpha_e (d\bar{X}_f/dt) \bar{X}_f \, dt}$$

Solving the same, we have:

$$c = \left[1 + \frac{\rho_a}{\rho_s}\frac{\alpha_e}{\bar{Q}_s}\frac{\bar{X}_f{}^2}{2}\right]^{-1} \tag{3.3}$$

The above equations are simple algebraic expressions and can easily be solved by substituting values of the variables at time step $t + 1$. Similarly, ρ_c can be determined by algebraically solving Eq. (2.23) after substitution of c and T_c at $t + 1$. Thus, ρ_c is defined as:

$$\frac{\rho_a}{\rho_c} = \left[(1 - c) + c\frac{R_s}{R_a}\right]\bar{T}_c \tag{3.4}$$

The frontal velocity of the cloud (U_f) can be obtained from Eq. (2.24) (reprinted below) upon substituting values of c, ρ_c and X_f at time step $t + 1$.

$$\bar{U}_f = Fr\left[\left|1 - \frac{\rho_a}{\rho_c}\right|\frac{1}{c}\frac{\bar{Q}_s}{\bar{X}_f}\right]^{1/2} \tag{3.5}$$

The top entrainment velocity is calculated from the expression selected for the phenomenon of entrainment. Since entrainment is assumed to be proportional to the frontal velocity, the entrainment velocity is given by the simple relationship below:

$$\bar{v}_e = \alpha_e \bar{U}_f \tag{3.6}$$

Finally, the relation to determine advection velocity given by Eq. (2.26) can also be solved by the Runge-Kutta method to determine U_c, after expanding it to the standard form as shown below:

$$\overline{V\rho_c}\frac{d(\bar{U}_c)}{d\bar{t}} = \bar{\rho}_a\frac{d\bar{V}}{d\bar{t}}\left(\frac{\beta_c\bar{U}_w + \bar{U}_c}{2}\right) - \overline{VU_c}\frac{d\bar{\rho}_c}{d\bar{t}} - \overline{\rho_c U_c}\frac{d\bar{V}}{d\bar{t}} \tag{3.7}$$

Here, the cloud density and cloud volume differential is obtained from their respective values at current and earlier time steps as described below.

$$\frac{d\bar{\rho}_c}{d\bar{t}} = \frac{\overline{\rho_{c(t+1)}} - \overline{\rho_{c(t)}}}{\Delta t}$$

and

$$\frac{d\bar{V}}{d\bar{t}} = \frac{\bar{V}_{(t+1)} - \bar{V}_{(t)}}{\Delta\bar{t}} = \frac{\bar{\rho}_s\bar{Q}_s}{\Delta\bar{t}}\left(\frac{1}{c_{(t+1)}\overline{\rho_{c(t+1)}}} - \frac{1}{c_{(t)}\overline{\rho_{c(t)}}}\right)$$

Thus, we can solve for the cloud variables in a time incremental fashion with the help of the above seven equations for a numerical solution. Though this process can be carried out by manual calculations, it would be a time-intensive and error-prone procedure. It would be best to program a computer to carry out the exhaustive calculations and their repetitive cycles. There already exist programs in various computer languages to carry out the Runge-Kutta fourth order scheme; for example, the site http://nacphy.physics.orst.edu/ComPhys/DIFFEQ/mydif2 on the Internet and Viscous fluid flow [15].

4. Results and discussion

The model has been executed for varied input data to ascertain the trends in the cloud variables. Trial runs have been carried out to analyze the behavior of the cloud under varied source and/or environmental conditions. This section deals with the plotting of the results obtained and its study. This is useful in drawing suitable conclusions regarding the qualitative and quantitative behavior of the model.

Model evaluation involves the comparison of the model results to observed trends and available data to estimate the accuracy of the model predictions and verify the general model behavior. The model developed is compared to cloud characteristic behavior and observed dispersion trends by carrying out runs using standard input values and plotting the resulting output parameters. To compare the model trends the values for most of the input variables are the same as in those in trial runs by Kunsch and Fannelop [7] for a cold (liquefied) nitrogen cloud released instantaneously with $\rho_a = 1.2\,kg/m^3$, $\rho_s = 1.87\,kg/m^3$, $h_0 = 1.09\,m$, $X_{f_0} = 1.82\,m$, $T_a = 500\,K$, $T_s = 300\,K$, $\varepsilon = 0.001$ with $U_w = 0.007\,m/s$. The appropriate output plots obtained, after executing the developed model for the standard input values, are given in Figs. 3–8 and are discussed below.

The plot of cloud length versus time (Fig. 3) indicates the expected trend of increasing cloud length with time. However, one should bear in mind that the model has been developed

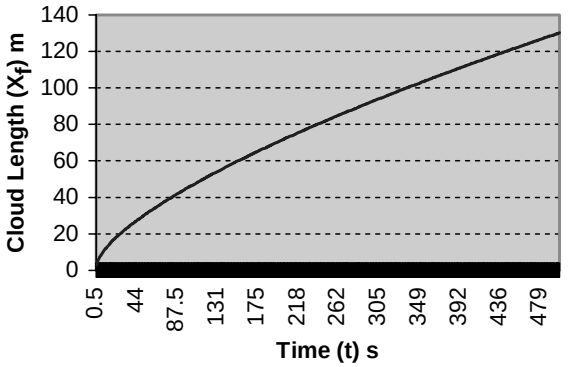

Fig. 3. Cloud length vs. time for standard values.

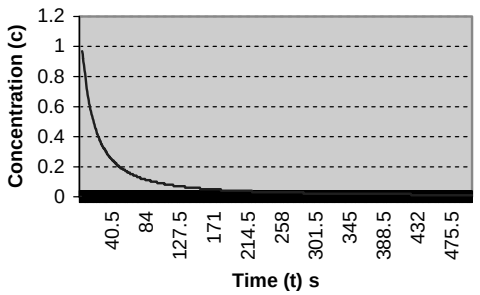

Fig. 4. Concentration vs. time for standard values.

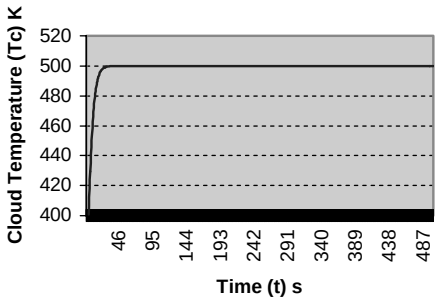

Fig. 5. Cloud temperature vs. time for standard values.

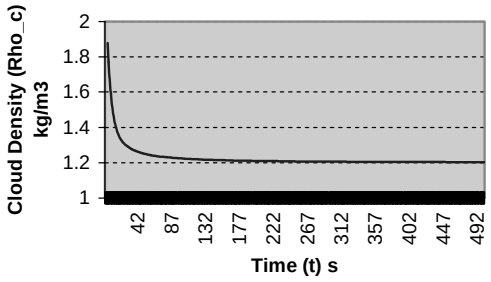

Fig. 6. Cloud density vs. time for standard values.

for early stages of cloud dispersion hence the trailing values may not be representative of observed behavior. The plot of concentration versus time (Fig. 4) also shows observed behavior of decreasing concentration with time. We notice that the concentration drops drastically in the early stages of dispersion, which agrees with the observed increase in length of cloud and sharp drop in density. The concentration approaches zero at long times. The cloud temperature is observed to reach ambient temperatures in the very early stages from the model run (Fig. 5). Though a similar trend is observed by Kunsch and Fannelop

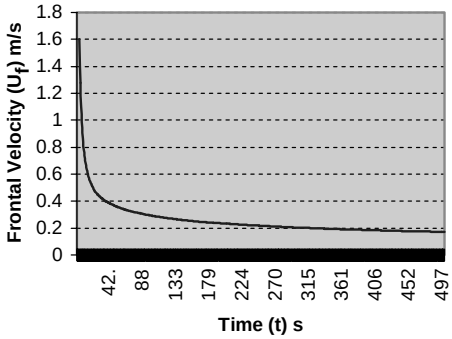

Fig. 7. Cloud frontal velocity vs. time for standard values.

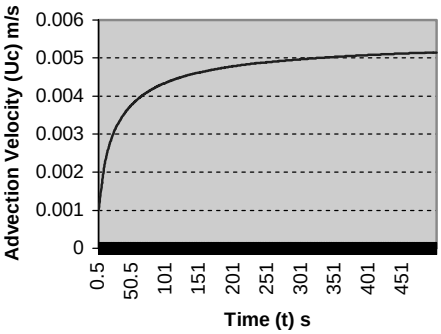

Fig. 8. Advection velocity vs. time for standard values.

[7] model, the rate of temperature increase is less compared to the present model, partly because of the constant rate of entrainment assumed in the former model. The plot for rate of change of cloud density, Fig. 6, resembles the plot of concentration and approaches the ambient density, as the cloud becomes a passive one. The cloud frontal velocity (Fig. 7) decreases rapidly and then becomes stable indicating that after the early stages of cloud expansion, the cloud continues to expand at a slower pace. Finally, on observing the plot for advection velocity versus time (Fig. 8), we notice a steady increase in advection velocity till it reaches a fraction of the ambient wind velocity prevalent.

The model is also evaluated for the effects of heat on dispersion of the cloud. The model is run for the scenario where no heat transfer occurs by equating the temperature of the source to ambient temperature. Figs. 9–13 plot the results obtained from the run where most of input parameters are the same as that for the standard run described earlier except for the source temperature. The value of the source temperature at initial condition is the same as the ambient air temperature and Stanton number is equal to zero. On comparing Figs. 3–9, we notice that the cloud length has increased in the case of no-heat transfer. This result accurately matches the trend shown in Figs. 3 and 4 of Kunsch and Fannelop [7]. As a direct result of larger increase in cloud length for no heat transfer case, we notice that concentration (Fig. 10) decreases more rapidly than in case of heat transfer (Fig. 4). The plots for density versus time (Figs. 11 and 6) show nearly the same behavior for both runs,

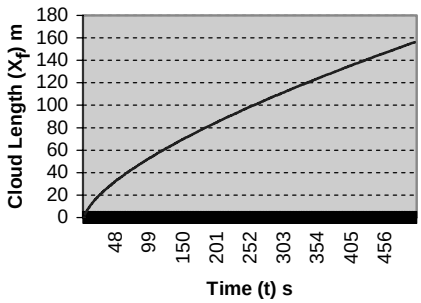

Fig. 9. Cloud length vs. time for no heat transfer.

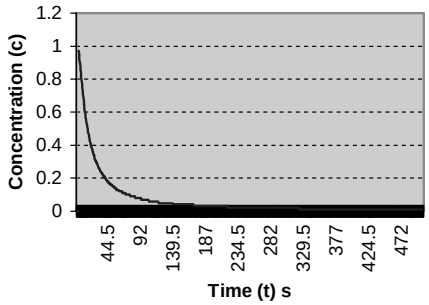

Fig. 10. Concentration vs. time for no heat transfer.

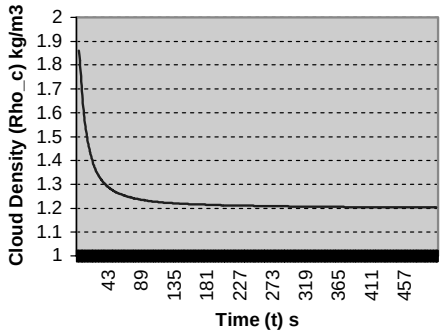

Fig. 11. Cloud density vs. time for no heat transfer.

approaching ambient density at nearly same times. The frontal velocity in case of no heat transfer (Fig. 12) is observed to decrease at a slower rate than in the case where heat transfer (Fig. 7) exists. This result also compares well with observed data and Kunsch and Fannelop model [7] results. There is no apparent difference in behavior of advection velocity (Figs. 13 and 8) under the two differing heat transfer conditions because a low value of atmospheric wind velocity (0.007 m/s) was used for the run.

The input parameters for the box model that has been developed include various source

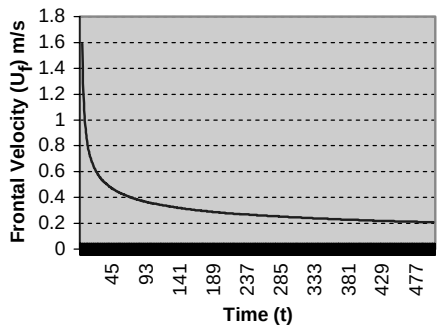

Fig. 12. Frontal velocity vs. time for no heat transfer condition.

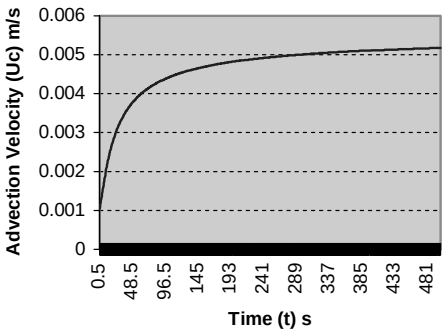

Fig. 13. Advection velocity vs. time for no heat transfer condition.

characteristics and environmental conditions which affect the properties of the cloud. The study of the effect of variation of these parameters on the cloud dispersion helps in understanding the underlying phenomena in a heavy-gas dispersion model and also helps in predicting the cloud behavior under different conditions. The source characteristics like density, specific heat capacity, temperature and environmental conditions like Stanton number (*St*), ambient temperature, wind speed, conductivity of the ground, etc., affect the cloud properties to varying degrees. The influence of some of the above parameters on the behavior of cloud has been analyzed to better understand its behavior as explained below:

- The analysis of model behavior for varying densities indicated an increase in the cloud length with an increase in source density (Fig. 14). Other parameters, like cloud

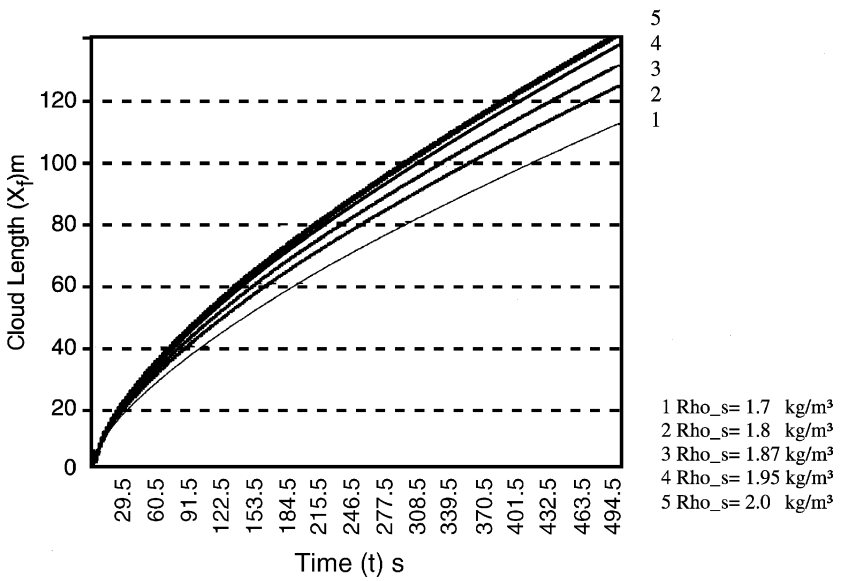

Fig. 14. Cloud length vs. time for varying source density.

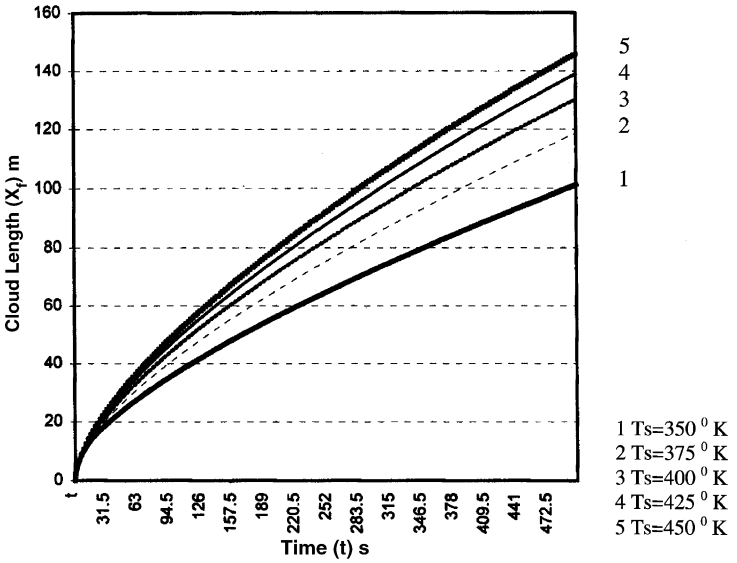

Fig. 15. Cloud length vs. time for varying initial cloud temperature.

temperature, concentration and velocity, showed a negligible effect to changes in density. This increase in cloud length may partially be attributed to decrease in cloud height due to heavy nature of dispersing gas.

- The behavior of cloud for changing initial cloud temperatures indicated a greater rate

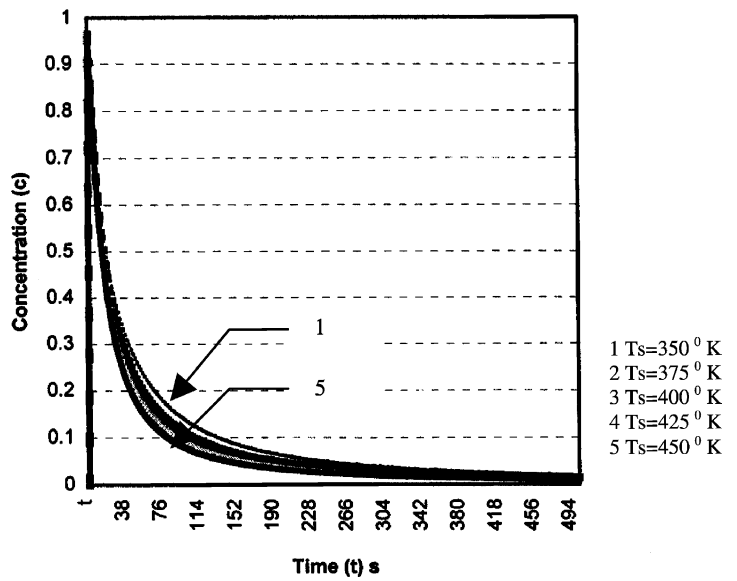

Fig. 16. Concentration vs. time for varying initial cloud temperature.

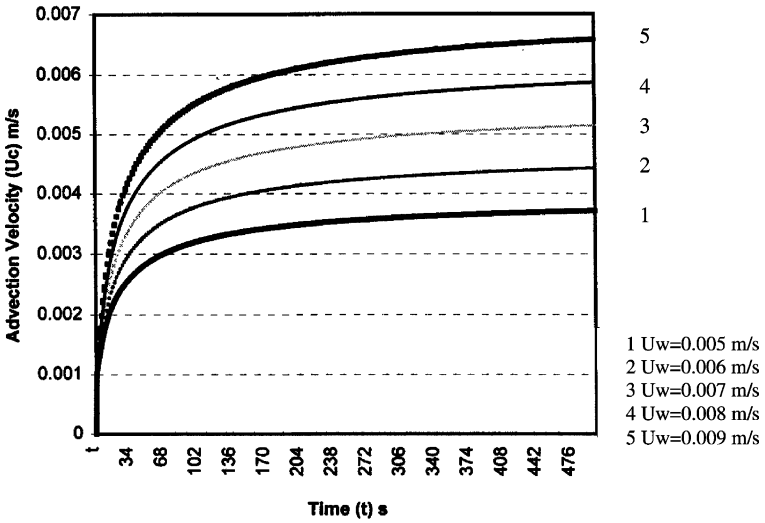

Fig. 17. Advection velocity vs. time for varying wind velocity.

of cloud spreading for higher temperatures (Fig. 15). The rate of drop in concentrations was observed to be more rapid for hotter clouds (Fig. 16). However, cloud density and velocity indicate negligible effects of initial temperature on their behavior. In summary, a warmer cloud is expected to disperse faster.

- Advection velocity, being a function of wind velocity, increases with increasing ambient velocities and gradually stabilizes to a fraction of the ambient speed (Fig. 17).

A sensitivity analysis of the proposed model was carried out by Kumar et al. [16]. They concluded that four input parameters show Type III sensitivity based on ASTM guidelines [17] towards the observed output of cloud length, concentration, and cloud temperature (Table 1).

Future work should be carried out to improve algorithms for advection velocity and cloud entrainment.

Table 1
Summary of sensitivity results from Kumar et al. [16]

Input parameter	Output parameter			
	Concentration	Cloud length	Cloud temperature	Advection velocity
Surface temperature	Type III in early stages, Type I in later stages	Type III	Type III in early stages, Type I in later stages	Type I
Source density	Type III for lower densities, Type I for higher densities	Type III	Type III in early stages, Type I in later stages	Type I
Initial cloud length	Type III in early stages, Type I in later stages	Type III	Type III in early stages, Type I in later stages	Type I
Initial cloud height	Type III in early stages, Type I in later stages	Type III	Type III in early stages, Type I in later stages	Type I

5. Conclusions

A model for the release of instantaneous heavy gas release in a channel (one horizontal dimension) incorporating surface heat transfer was developed. The model results were analyzed qualitatively and quantitatively, in order to use the model for prediction purposes.

References

[1] R.E. Britter, Atmospheric dispersion of dense gases, Ann. Rev. Fluid Mech. 21 (1989) 317–344.
[2] R. Bellasio, M. Tamponi, MDGP: a new Eulerian 3D unsteady state model for heavy-gas dispersion, Atmos. Environ. 28 (9) (1994) 1633–1643.
[3] S.R. Hanna, D.G. Strimaitis, J.C. Chang, Evaluation of 14 hazardous gas models with ammonia and hydrogen fluoride field data, J. Hazard. Mater. 26 (1991) 127–158.
[4] C.S. Matthais, Dispersion of a dense cylindrical cloud in a turbulent atmosphere, J. Hazard. Mater. 30 (1992) 117–150.
[5] J.P. Kunsch, D.M. Webber, Simple box model for dense-gas dispersion in a straight sloping channel, J. Hazard. Mater. A75 (2000) 29–46.
[6] V. Gudiwaka, Evaluation of four box models for instantaneous dense gas releases, M.S. Thesis, University of Toledo, Toledo, 1989.
[7] J.P. Kunsch, T.K. Fannelop, Unsteady heat-transfer effects on the spreading and dilution of dense gas clouds, J. Hazard. Mater. 43 (1995) 169–193.
[8] P.W.M. Brighton, A.J. Byrne, R.P. Cleaver, P. Courtiade, B. Crabol, R.D. Fitzpatrick, A. Girard, S.J. Jones, V. Lhomme, A. Mercer, D. Nedelka, C. Proux, D.M. Webber, Comparison of heavy-gas dispersion models for instantaneous releases, J. Hazard. Mater. 36 (1994) 193–208.
[9] C.J. Wheatley, P.W.M. Brighton, A.J. Prince, Comparison between data from the heavy-gas dispersion experiments at Thorney Island and predictions of simpler models, in: Proceedings of the Fifteenth International Technical Meeting on Air Pollution Modeling and It's Applications, NATO/CCMS, St. Louis, MO, USA, Paper VI.5, 1985.
[10] C.J. Wheatley, A.J. Prince, Translation cloud speeds in the Thorney Island trials: mathematical modeling and data analysis, J. Hazard. Mater. 16 (1987) 185–199.
[11] M. Nielsen, S. Ott, Heat transfer in large-scale heavy-gas dispersion, J. Hazard. Mater. A67 (1999) 41–58.
[12] J.A. Fay, D. Ranck, Scale Effects in Liquefied Fuel Vapor Dispersion, US Department of Energy Report, DOE-EP-0032 UC11, 1981.
[13] A.P. Van Ulden, The unsteady gravity spread of a dense cloud in calm environment, in: Proceedings of the Tenth International Technical Meeting on Air Pollution Modeling and It's Applications, NATO-CCMS, Rome, Italy, 1979.
[14] A.E. Germeles, E.M. Drake, Gravity spreading and atmospheric dispersion of LNG vapor clouds, in: Proceedings of the Fourth International Symposium on Transport of Hazardous Cargo by Sea and Inland Waterway, Jacksonville, Florida, 1975.
[15] F.M. White, Viscous fluid flow, in: McGraw-Hill Series in Mechanical Engineering, McGraw-Hill, New York, 1991.
[16] A. Kumar, A. Mahurkar, A. Joshi, Sensitivity analysis of an instantaneous Box Release Model with surface heat transfer, in: Proceedings of the 2001 Annual Conference, A&WMA, Orlando, FL, USA, Paper 42755, 2001.
[17] ASTM, Standard Guide for Conducting a Sensitivity Analysis for a Ground-Water Flow Model Application, ASTM Designation: D 5611-94, 1994.